

Degradation of nickel anodes in alkaline fuel cells

M. Schulze*, E. Gülzow

Institut für Technische Thermodynamik, Deutsches Zentrum für Luft- und Raumfahrt e.V., Pfaffenwaldring 38–40, D-70569 Stuttgart, Germany

Abstract

Alkaline fuel cells (AFC) are an interesting alternative to polymer electrolyte fuel cells (PEFC), especially AFCs need neither expensive electrolytes nor expensive noble metal catalysts. For using of AFCs long-term stability of the components is decisive, in particular the stability of the electrodes, because the electrolyte can be easily exchanged.

The long-term behavior of AFC anodes was investigated electrochemically by measuring $U-i$ curves. The electrodes consisting of a mixture of a nickel catalyst, which is formed from an aluminium–nickel alloy by dissolving the aluminum, polytetrafluorethylene (PTFE) as organic binder and with added copper powder, rolled onto a metal web. In addition, these electrodes were characterized physically after different operation times by X-ray photoelectron spectroscopy (XPS), porosimetry measurements by nitrogen adsorption, scanning electron microscopy (SEM) and energy dispersive X-ray analysis (EDX).

The electrochemical performance decreases with operating time. The decrease of the electrochemical performance can be described by combination of two exponential functions with different time constants. The physical characterization shows that the PTFE in the electrodes partially decomposes and the nickel catalysts disintegrates. The changes of the physical characteristics can be correlated with the electrochemical performance.

© 2003 Elsevier B.V. All rights reserved.

Keywords: Alkaline fuel cells; X-ray photoelectron spectroscopy; Polytetrafluorethylene; Degradation; Nickel electrodes

1. Introduction

Fuel cells have the potential to become an important technology in future with the highly efficient generation of electrical power. Low temperature fuel cells such as polymer membrane fuel cells (PEFC), direct methanol fuel cells (DMFC), and alkaline fuel cells (AFC) as well are considered as promising options for powering future cars [1,2] and small combined power units due to their modular construction and the high energy densities that can be attained. At present, the polymer electrolyte membrane fuel cells (PEFC and DMFC) are preferred, but like every fuel cell the PEFC has specific advantages and disadvantages. One advantage of AFC is that no expensive noble metals are required as catalyst, because of the lower corrosivity of the catalyst and a higher catalytic activity for the oxygen reduction reaction in a basic environment compared to an acidic one. Nickel can be used as catalyst in the anode and silver in the cathode. On the surface of the anode, hydrogen is able dissociate and to adsorb ($H_{2\text{gas}} \rightarrow 2H_{\text{adsorbed}}$). Also hydroxide ions from the

alkaline solution adsorb on the anode surface, whereby the ions transfer their electrons to the anode surface ($2OH^- \rightarrow 2OH_{\text{adsorbed}} + 2e^-$). The adsorbed hydroxide groups and the adsorbed hydrogen reacts and forms water, which desorbs from the anode catalyst surface ($OH_{\text{adsorbed}} + H_{\text{adsorbed}} \rightarrow H_2O$). On the cathode, the oxygen adsorbs and dissociates on the cathode catalyst surface ($O_2 \rightarrow 2O_{\text{adsorbed}}$). In the basic environment, the dissociation of the oxygen is not hindered as it is in an acidic environment. The adsorbed oxygen polarizes the cathode surface by a partial transfer of the charge to the adsorbed oxygen. In addition, the adsorption of water on the cathode is also necessary. Some of the adsorbed water molecules dissociate on the surface whereby, the formed adsorbed hydrogen reacts with the adsorbed oxygen forming hydroxide groups ($O_{\text{adsorbed}} + H_2O \rightarrow 2OH_{\text{adsorbed}}$). The residual adsorbed water forms a water shell around the OH groups and allows the transfer of an electron from the catalyst to the hydroxide group and the desorption from the surface ($OH_{\text{adsorbed}} + e^- \rightarrow OH^-$).

An other advantage of the AFC compared with PEFC is that the liquid electrolyte can be used for the regulation of the temperature in the fuel cell and does not need extra cooling cells like the PEFC, although the liquid electrolyte is more corrosive compared to water in the cooling circuit in

* Corresponding author. Tel.: +49-711-6862-456;
fax: +49-711-6862-332.
E-mail address: mathias.schulze@dlr.de (M. Schulze).

PEFCs. In addition to the named advantages of AFC, it does not need a humidification of the process gases. The low CO₂ tolerance of AFC is frequently named as the main problem of AFC systems; an investigation of the CO₂ tolerance of AFC is given in [3], which shows that in fact an AFC system shows a high CO₂ tolerance. An alternative for the PEFC systems is the alkaline fuel cell, whereby the AFC research and development reached its peak in the beginning of the 1980s, so the AFC has the potential as an alternative to the PEFC if the progress of science and technology within fuel cells will be also used for AFC.

Besides the costs of fuel cells, their lifetime is a general problem for their technical use in stationary or mobile applications. During lifetime, the fuel cell performance and behavior should not change significantly. The end of the lifetime is determined by changes of fuel cell components, which results eventually in a considerable decrease of the electrochemical performance. To understand this decrease, knowledge about the changes of the fuel cell components and their consequences, as well as the understanding of the influence of the changes of the individual components on the fuel cell operation are necessary. Therefore, studying the changes of individual fuel cell components is the first step to investigate the degradation of fuel cells. The alkaline fuel cells can be dismantled without any problem into the components, which allows investigation of the components with a lot of different methods. This is a significant advantage for the study of degradation processes, but only few studies on the electrochemically induced changes of AFC components exist [4–12]. The degradation of three different anode types prepared in similar way are described in [12], and the present paper is focussed on the anode type, which is named in [12] as type 2.

These electrodes consist of a Raney-nickel catalyst, added copper powder and polytetrafluorethylene (PTFE) on a metal web. During operation time, a decrease of the electrochemical performance was observed [8,11]. The physical characterization of the electrodes after operation shows that the pore size distribution has changed [11], whereby the specific surface remained almost unchanged. The nickel catalyst particles were disintegrated during electrochemical operation. If the anodes are overloaded, so that the polarization of the electrodes is high, the nickel will be oxidized [8]. The copper is partially dissolved in the electrolyte. Residual aluminum content will be further dissolved during fuel cell operation [8]. The PTFE is altered by the electrochemical stressing [7]. This result is very surprising because PTFE should be stable in all electrochemical conditions.

The same effects are also observed during the activation process of the electrodes [10], e.g. dissolving of the copper, whereby the copper is transported through the surface to the electrolyte. In X-ray photoelectron spectroscopy (XPS) measurements, a change of the copper concentration on the electrode surface was observed which depends on time and current density.

2. Experimental

2.1. Electrode preparation

The investigated anodes consist of a metallic catalyst, PTFE, and added copper on a metal web. The catalyst is necessary for the electrochemical reaction and the electrical conduction to the metal web. The metal web serves as a stable carrier for the electrode and for the electric conduction. The PTFE is hydrophobic, and thus prevents the electrode from being totally flooded by the electrolyte which penetrates into the pore system. It also allows the gas transport into the electrode; consequently the three-phase zone, where the electrochemical reaction takes place, is not only on the electrode surface but also formed in the volume of the electrodes. In addition, the PTFE works as an organic binder fixing the catalyst particles within the electrode.

The preparation of the gas diffusion electrode based on Sauer [13] and Winsel [14] has been further developed for electrodes of different low-temperature fuel cell types, alkaline fuel cells [15–21], and polymer electrolyte membrane fuel cells [22–26]. The investigated anodes consist mainly of a mixture of Raney-nickel catalyst with an addition of copper powder and PTFE powder on a copper web. The structure of the Raney-nickel catalyst is a highly porous arrangement of metal particles which are formed from an aluminium–nickel alloy by dissolving the aluminium.

The basic alloy used for the catalyst and the PTFE powder is the same for all electrodes. The preparation of the electrodes is described in more detail in [12]. The electrodes were activated in a standard procedure by hydrogen evolution at 5 mA/cm² for 18 h in a 30% KOH [10]. During this activation procedure, the oxidized nickel surface was reduced to metallic nickel, the copper was partially dissolved, the specific surface area increased, and the pore size distribution altered [10].

2.2. Electrochemical operation conditions and characterization

The anodes were electrochemically stressed and characterized in an electrochemical half cell configuration consisting of the electrode in a holder manufactured from plexiglass, a nickel counter electrode and a Hg/HgO reference electrode. In the experimental setup, the electrodes were supplied with pure hydrogen at ambient pressure from the backside, facing the metallic web. The electrode holder was inserted into a tempered vessel (353 K) containing 30% KOH. The electrodes have an active area of 6 cm².

The electrodes were loaded at various current densities from a low current density of 25 mA/cm² up to overloading of the electrodes (400 mA/cm²), whereby the electrode polarization reached the potential range where nickel oxide is formed. For the electrochemical characterization, *U*–*i* curves were recorded and corrected by *I*–*R* drop measurements to

compensate for the ohmic losses in the measured potential. The $U-i$ curves were recorded every 24 h.

2.3. Physical characterization of the electrodes after electrochemical operation

The electrodes were removed from the testing setup to perform the surface analysis. After removal from the half cell configuration, the electrodes were rinsed with distilled water. Subsequently, the electrodes were split in to different samples for different characterization methods and individually dried under the conditions, required for the specific analyzing method. For each measurement a new electrode was used. The electrodes were characterized by X-ray photoelectron spectroscopy to analyze the chemical composition of the surface [27], scanning electron microscopy (SEM) with energy dispersive X-ray spectroscopy (EDX) [27] to determine the structure and element distribution, and nitrogen adsorption [28] to investigate the pore size distribution. Different parts of the investigated gas diffusion electrodes (GDE) were dried before being analyzed under typical conditions. The sample preparation and the equipment used for the physical characterization of the anodes is described in [12].

3. Results and discussion

All electrodes have nearly the same initial electrochemical performance after their activation. An identical performance was also observed in $U-i$ curves of new anodes, prepared without copper powder but using the identical Raney-nickel catalyst [12]. To describe the long-term behavior of the electrochemical performance, we defined a parameter called surface specific conductivity. For low current densities, the $U-i$ curve has nearly a linear shape. The slope of the $U-i$ curve was defined as surface specific conductivity [12]. The current density divided by the polarization at 100 mV overvoltage gives almost the same value. In this definition, a high surface specific conductivity means a high electrochemical performance, and a decrease is related to a decrease of the electrochemical performance. A typical $U-i$ curve is given in [12]. The reciprocal gradient of the fitted straight line is the surface specific conductivity and is used as parameter for the electrochemical performance.

For the long-term behavior of the electrodes, experiments with different electrochemical loadings were performed. Electrodes were loaded with current densities from 25 mA/cm² up to 400 mA/cm², whereby long-term tests were performed at 25, 50, 100, 150 and 200 mA/cm².

The initial electrochemical performance of different samples of one electrode type differs by less than 20%, which can be explained by achieving different electrochemical active areas after the activation procedure. Fig. 1 shows the decrease of the electrochemical performance caused by electrochemically stressing at different current densities. In Fig. 1(a–e), the time curves of the electrochemical

performance have been normalized to the different initial electrochemical performance values to compare the different samples.

The time-dependent electrochemical performance for all shown current densities can be described by the combination of two exponential functions of the following form:

$$\text{Perf}(t) = a \exp\left\{-\frac{t}{t_0}\right\} + b \exp\left\{-\frac{t}{t_1}\right\} + c \quad (1)$$

Some of the four constants in the function (a , b , t_0 , and t_1) are variables, depend on the current density. For the investigated electrodes, stressed at constant loading, for one term of Eq. (1) one of the time constants t_0 was also determined to be approximately 200–250 h. For other similar anodes, using also a Raney-nickel catalyst at the same operation conditions and current density, the decrease of the electrochemical performance can be described by one exponential function with the same time constant [12].

The time constants were determined from the long-term behavior of the electrochemical performance operating under various electrochemical loadings. Both values for the various current densities are shown in Fig. 1f. One of the time constants, t_0 is independent from the current density in contrast to the second one t_1 , which strongly depends on the current density and varies over more than four orders of magnitude. The first-order regression used, related to an exponential dependence, does not fit very well but shows the strong influence of this parameter. The time dependence of the electrochemical performance must be described by both a current density independent term and a term that is depending on the current density, forming Eq. (2):

$$\begin{aligned} \text{Perf}(t) &= a \exp\left\{-\frac{t}{t_0}\right\} + b \exp\left\{-\frac{t}{t_1(i)}\right\} + c \\ t_1 &= t_{10} \exp\left\{-\frac{i}{i_0}\right\}, \quad t_{10} \approx 250 \text{ h}, \\ i_0 &\approx 25 \text{ mA/cm}^2, \quad t_{10} = 40,000 \text{ h} \end{aligned} \quad (2)$$

The equation for the time constant t_1 gives the dependence on the current density, so the Eq. (2) can be used at various constant loadings. Based on the Eq. (2) the time depending electrochemical performance of the investigated anodes under dynamic loading can be approximately described by the Eq. (3):

$$\begin{aligned} \text{Perf}(t) &= a \exp\left\{-\frac{t}{t_0}\right\} + b \int_0^t \left(t_{10}^{-1} \exp\left\{\frac{i(t')}{i_0}\right\} \right. \\ &\quad \left. \times \exp\left\{-\frac{t'}{t_{10}}\right\} \exp\left\{\frac{i(t')}{i_0}\right\} \right) dt' \end{aligned} \quad (3)$$

An influence of the alteration of load is not considered in this equation, but may have an influence on the electrochemical performance.

In addition to the electrochemical investigations, the electrodes were characterized by different physical methods.

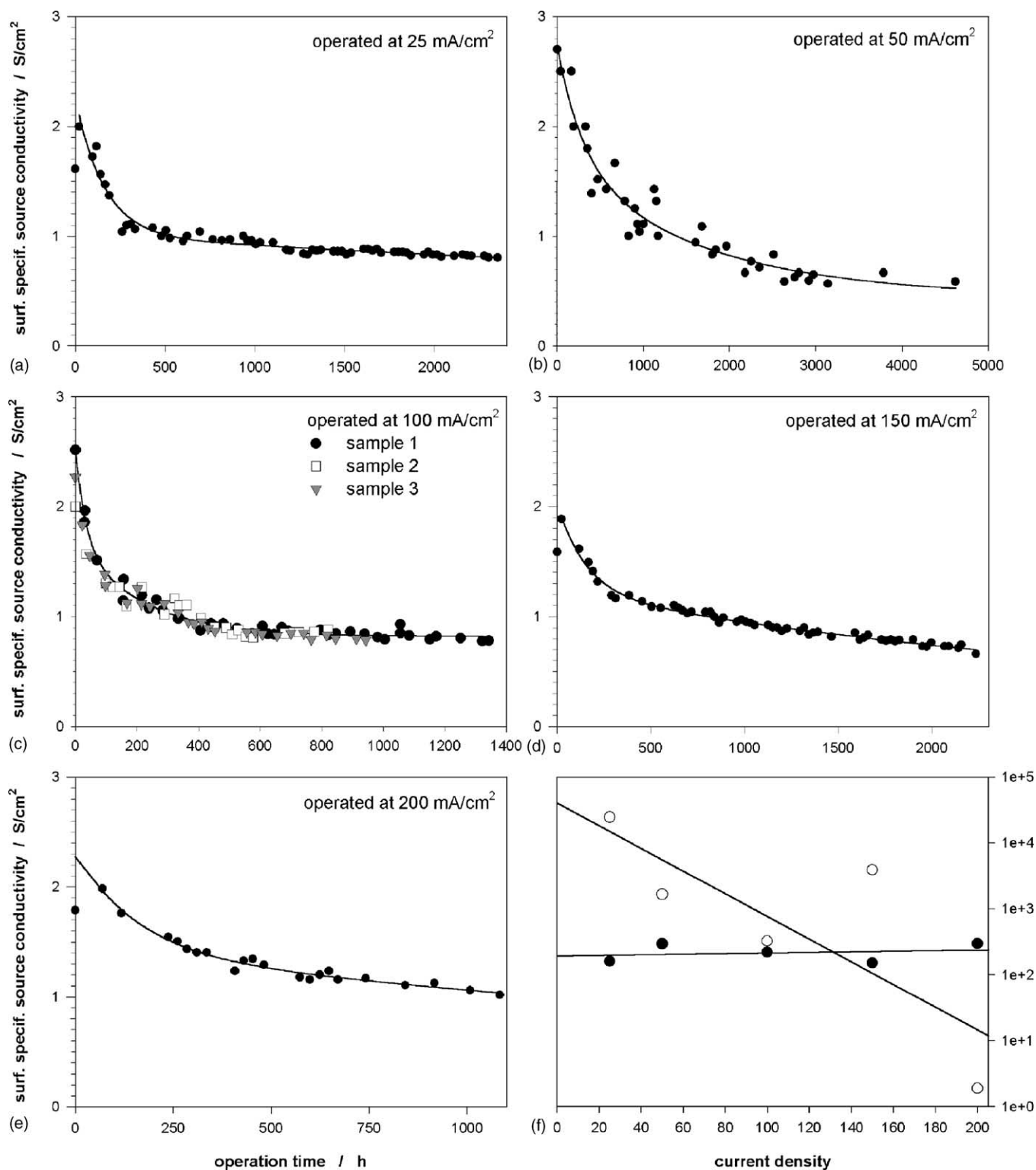


Fig. 1. Electrochemical performance during long-term experiments at various current densities: (a) 25 mA/cm², (b) 50 mA/cm², (c) 100 mA/cm², (d) 150 mA/cm², and (e) 200 mA/cm²; the symbols mark the measurement points, the straight lines are fitting curves with two exponential terms. Part (f) shows the dependence of the time constants (closed circles, t_0 and open circles, t_1) in the exponential functions on the current density.

X-ray photoelectron spectroscopy was used to investigate the changes in the chemical composition of the electrode surfaces. The physical characterizations were mainly performed with electrodes operated at 100 mA/cm² for various

operating times. The operating times varied between a fresh activated electrode to a long-term operation was 1344 h.

By successively recording of X-ray photoelectron spectra followed by ion etching of the surface, depth profiles were

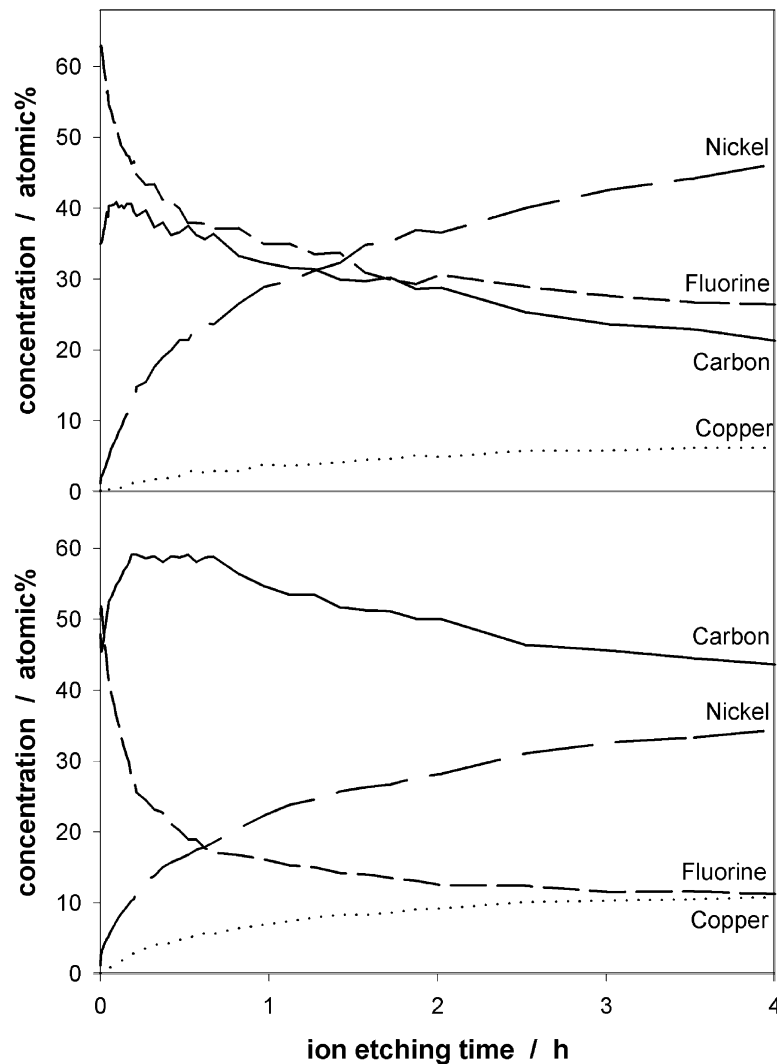


Fig. 2. Depth profiles measured by XPS of an activated electrode (on top) and of an electrode operated 1344 h at a current density of 100 mA/cm^2 (bottom).

measured up to a few nanometer. Fig. 2 shows depth profile measurements of a freshly activated anode and an anode which was electrochemically stressed at 100 mA/cm^2 for 1344 h. On the surface of both electrodes mainly carbon and fluorine are detected. The fluorine is bonded in the PTFE, the observed carbon signal can be partially related to the PTFE, whereas the residual carbon signal is related to PTFE fragments and organic impurities. In the XP spectra, different binding states and oxidation states can be distinguished by the binding energy of the photoelectrons, e.g. in the combination of fluorine and carbon the fluorine leads to a partial electron transfer from the carbon to the fluorine. In XPS investigation, such partial charge transfer results in a shift of the C 1s photoelectron peak to higher binding energies. During the depth profiling of both electrodes, the nickel catalyst, the added copper powder, carbon and fluorine from the PTFE were detected. In addition, carbon from organic impurities and the PTFE decomposition are also observed. In the depth profiles of both

electrodes, freshly activated and after operation, the main differences are observed in the concentrations of the nickel catalyst and of the PTFE components and decomposition products.

Decomposition of the PTFE in the electrodes under electrochemical conditions have been reported in previous studies [7,10,12]. The decomposition of the PTFE during the fuel cell operation can be seen in Fig. 3a, where the decreasing fluorine concentration is observed in the depth profiles after various operating times. Fig. 3a shows clearly that the fluorine concentration decreased during the operating time. During the decomposition of PTFE, the ratio between fluorine and carbon decreases and an increased fluorine-depleted fraction of PTFE is observed [7].

Alteration of the PTFE in the electrodes can influence the pore size distribution, similar to the activation process. During the activation of the electrodes, the change of the PTFE is one of the dominant processes. The pore system of the Raney-nickel catalyst of a freshly prepared electrode,

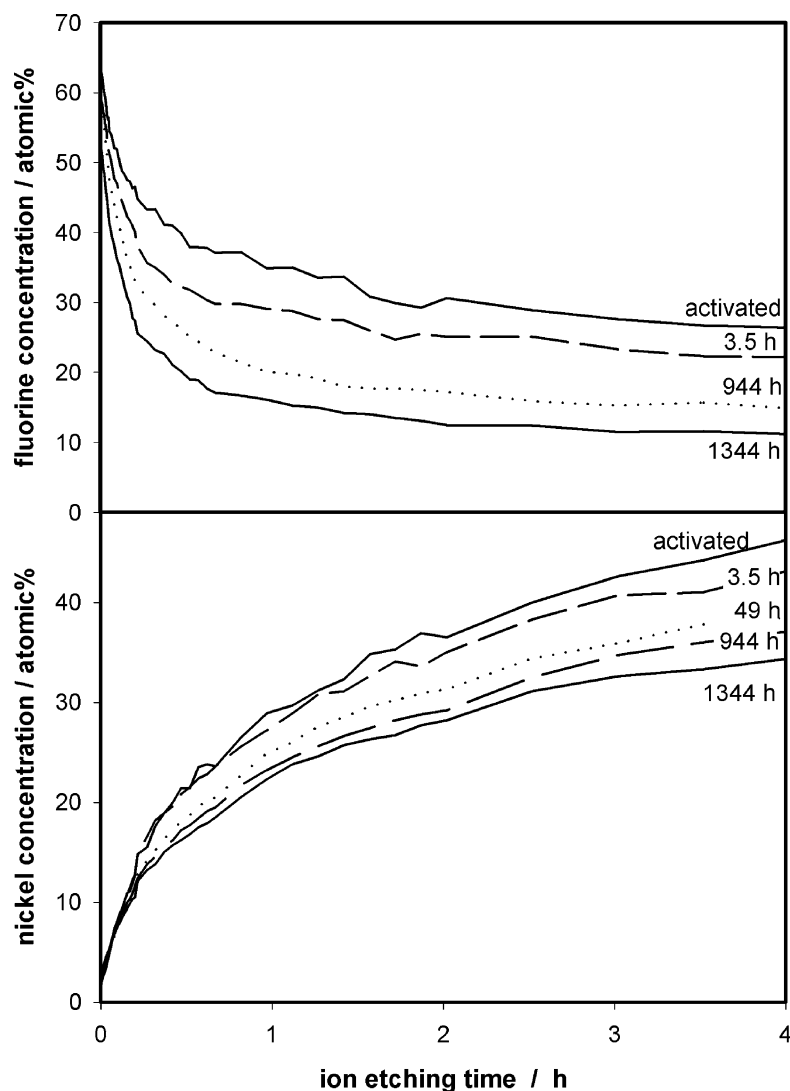


Fig. 3. Fluorine (on top) and nickel (bottom) concentrations recorded in the depth profile measurements of electrodes operating various periods at 100 mA/cm^2 .

covered by a PTFE film, is partially uncovered due to the activation process, which seems to be the time-dependent step of the activation process [10]. PTFE is hydrophobic and so it determines the intrusion of the electrolyte during the electrochemical operation, whereas the alteration of the PTFE can also change the electrochemical behavior. This will be described in a future paper [29].

Parallel to the decrease of the fluorine concentration in the electrode during operation, the nickel concentration increases, as shown in Fig. 3b. For all electrodes, the same shape of the depth profiles is observed but the nickel concentration in the electrodes decreases due to the electrochemical stressing. After 1344 h operating time, the nickel concentration at the end of the depth profiling is reduced by approximately 30% compared to the nickel concentration of the freshly activated electrode. The observed reduction of the nickel concentration is too small to explain the

significantly higher reduction of the electrochemical performance after 1344 h to approximately one-third of the initial performance (Fig. 1c).

The activity of the electrode is determined by the extension of nickel surface and its oxidation state in the three-phase zone. The three-phase region, where the reaction takes place, is formed by catalyst, gas phase, and electrolyte. Principally, the oxidation state of the nickel is determined by the electrochemical potential on the surface, but caused by dynamic effects in the three-phase zone the reaction zones can be moved by bubbles, changes in electrolyte concentration due to formation of reaction water and so on. The local electrochemical conditions in the electrodes are not homogeneous and can be significantly different from the overall conditions. In addition, some of the oxidation states of nickel are very stable and will not be reduced fast under reductive potential.

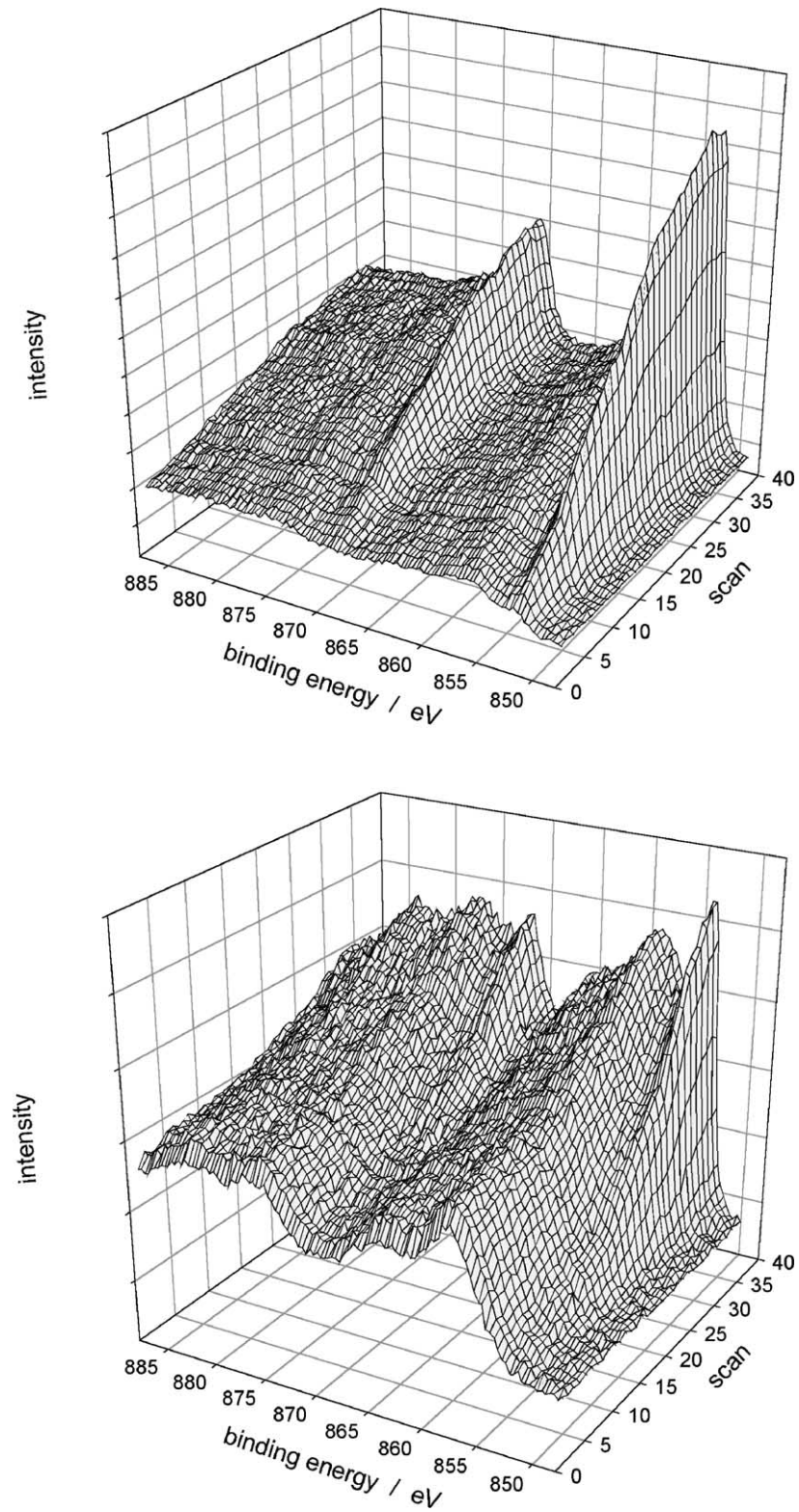


Fig. 4. Ni 2p spectra recorded during XPS depth profile measurements of an activated electrode (on top) and after long-term operation (approximately 5000 h) at 50 mA/cm² (bottom).

The different oxidation states of the nickel can be determined with XPS [30–32]. Fig. 4 shows the Ni 2p spectra recorded by XPS during depth profiling of an activated electrode and an electrode, which was electrochemically stressed at 50 mA/cm² for approximately 5000 h. The signal at 852.3 eV binding energy is related to the Ni 2p_{3/2} photoelectrons of metallic nickel, for NiO this signal is shifted to 853.3 eV binding energy. The signals of Ni 2p_{3/2} photoelectrons with higher binding energies are related to electrochemically formed nickel hydroxide and nickel oxy-hydroxide, Ni(OH)₂ and NiOOH. The increase of the nickel signal of the activated electrode during the depth profile measurements is correlated to the increase of the nickel concentration as shown in Fig. 2b. The spectra of the activated electrodes show mainly metallic nickel and a small contribution of nickel oxide, which is formed by the

reaction of adsorbed oxygen from the residual gas in the XPS system.

The long-term stressed electrode has low activity after 5000 h operation time, so that the electrode potential during operation was approaching the potential for the electrochemical formation of nickel oxides. The Ni 2p spectra of the electrodes show that the nickel catalyst is electrochemically oxidized. The nickel oxide does not support the hydrogen oxidation, and leads therefore to a decreasing electrochemical performance. At the end of life of the anodes, the formation of nickel oxides typically will be enhanced, caused by the increasing polarization. Consequently, due to the formation of nickel oxides the electrochemical performance continues to decrease and the polarization increases. This results in an accelerated formation of nickel oxides and a fast loss of the electrochemical performance at the end of

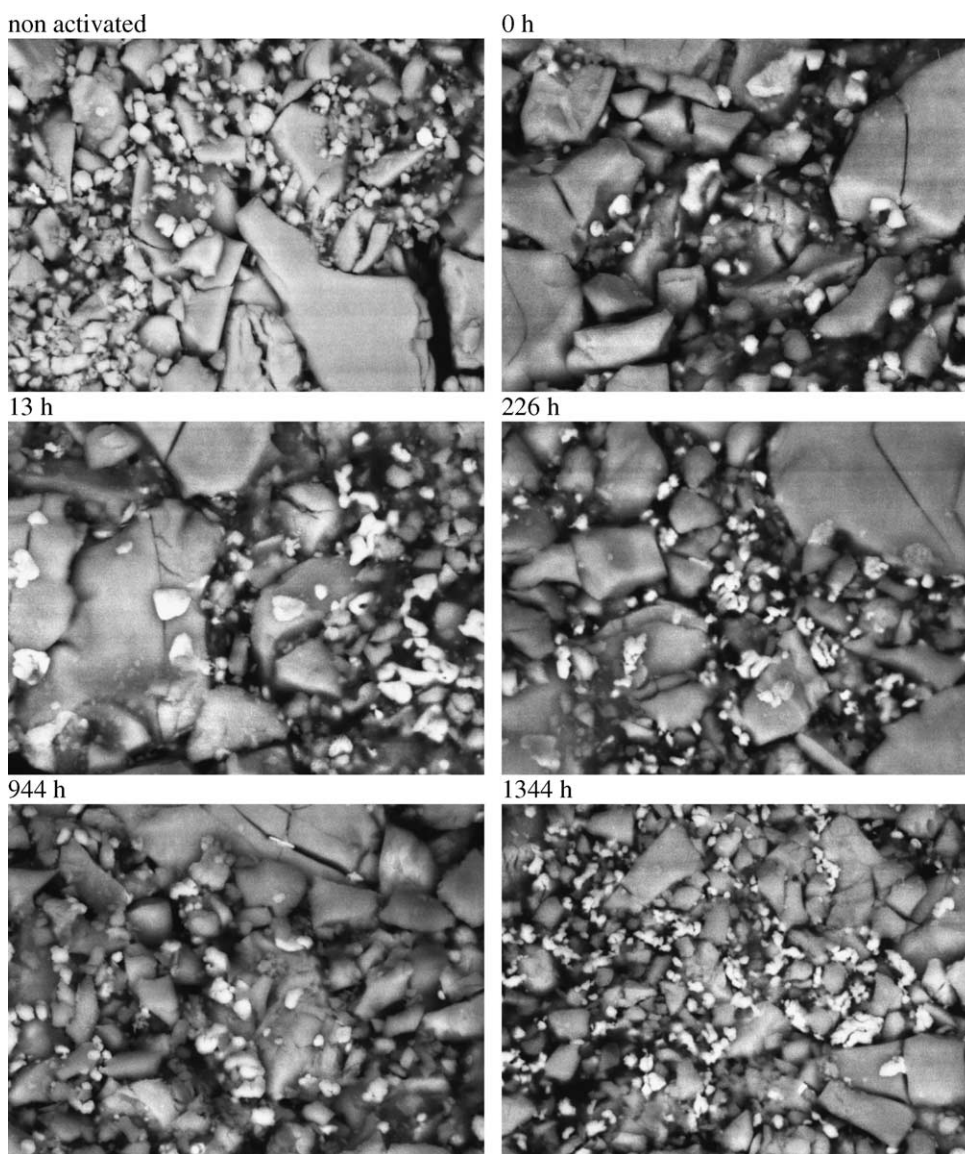


Fig. 5. SEM images of anodes unstressed and electrochemically stressed for various periods at a current density of 100 mA/cm². On top a non-activated (left) and an activated and operated electrode (right), below electrodes after 13, 226, 944, and 1344 h operation time.

the lifetime. This behavior is not shown in Fig. 1 because the electrochemical experiments were stopped before the electrodes became inactive, but this behavior was observed for electrodes loaded at higher current densities (400 mA/cm^2) in order to perform accelerated lifetime tests. The lifetime curve of another anode type up to the end of the lifetime is shown in Fig. 2 of [12].

In addition to analyzing the chemical surface composition of the electrodes, the structure was investigated by SEM. Fig. 5 shows the SEM images of electrodes which had been operated over various periods at 100 mA/cm^2 . The SEM measurements were performed using an electron beam voltage of 30 keV. As a consequence of the high beam voltage, the PTFE will not be imaged because of its transparency for high energy electrons. The small bright particles are related to copper powder, the larger less bright particles to nickel catalyst. This was proved by EDX measurements of single particles in the electrode. The comparison of both SEM images on the top shows that the concentration of the copper powder decreases due to the activation process, as described in [10]. The form and distribution of the nickel catalyst is not changed by the activation process. During the fuel cell operation of the anodes, the nickel particles become smaller; it seems that the large nickel particles are disintegrated to few smaller particles. The SEM images of the electrodes stressed for 13 h and for 226 h show that the disintegration process is not enhanced at the beginning of the electrochemical stressing. The disintegration of nickel particles can be explained by the well known hydrogen induced embrittlement of nickel.

In addition to the disintegration of the nickel catalyst, the mean size of the copper particles is also decreased, but from the SEM images it cannot be concluded that the copper particles are disintegrated in the same way. The copper particles size is reduced by partial dissolving of copper in the electrolyte. After long-term operation copper can be detected in the electrolyte.

The pore system of the electrodes measured by nitrogen adsorption is determined by the open pores in the nickel catalyst, therefore the disintegration of the nickel particles influences the pore size distribution.

Fig. 6 shows the pore size distribution of the electrodes, stressed at 100 mA/cm^2 for various periods, measured by nitrogen adsorption. A maximum in the pore size distribution around 2 nm can clearly be observed for all electrodes. The recorded pore system is related to the Raney-nickel catalyst [10]. During the fuel cell operation, the pore frequency at 2 nm increases as also shown in Fig. 7. The increase of the pore frequency can be effected by two mechanisms.

After the preparation of the electrodes, the surface of the electrode is covered by PTFE and will be partially uncovered by the activation procedure, so the pore frequency at 2 nm increases during the activation process [33]. Consequently, the observed decomposition of the PTFE during the fuel cell operation may induce the increase of the pore frequency. The second explanation of the increase of the pore frequency can

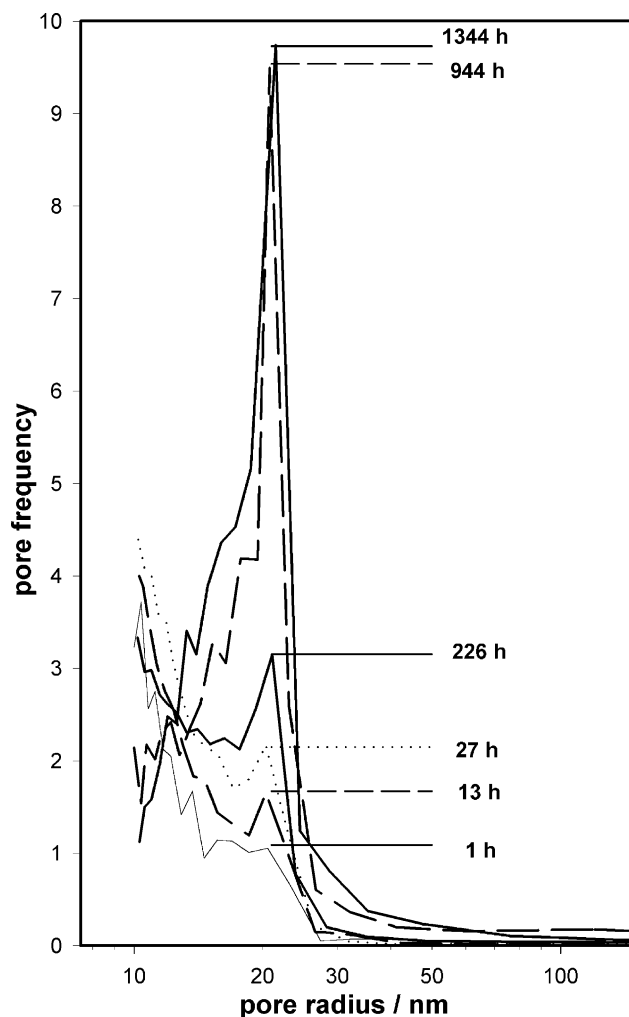


Fig. 6. Pore size distribution measured by nitrogen adsorption measurements of electrodes after various operation times at 100 mA/cm^2 .

be related to the disintegration of the nickel catalyst particles. Caused by the disintegration of the nickel particles, the inner pore system of the nickel particles will be accessible for the porosimetry measurements and so the measured pore frequency increases. Both effects—the decomposition of the PTFE and the disintegration of the nickel particles—should also have an effect on the measured specific surface area. The recorded specific surface area does not change significantly on the electrochemical stressing of the electrodes (Fig. 8). This is in contrast to the change of the specific surface area during the activation process, whereby the specific surface area increases corresponding to the pore frequency [10,33].

The specific surface area is the result of the complete pore system. If the disintegration of the nickel particles take place along wide pores, the specific surface area does not significantly increase but the pore frequency at 2 nm increases. The disintegration of the nickel particles along pores probably takes place in the grain boundaries of the single crystallites, which are at the end of the pores. The hydrogen induced embrittlement is enhanced at the grain boundaries

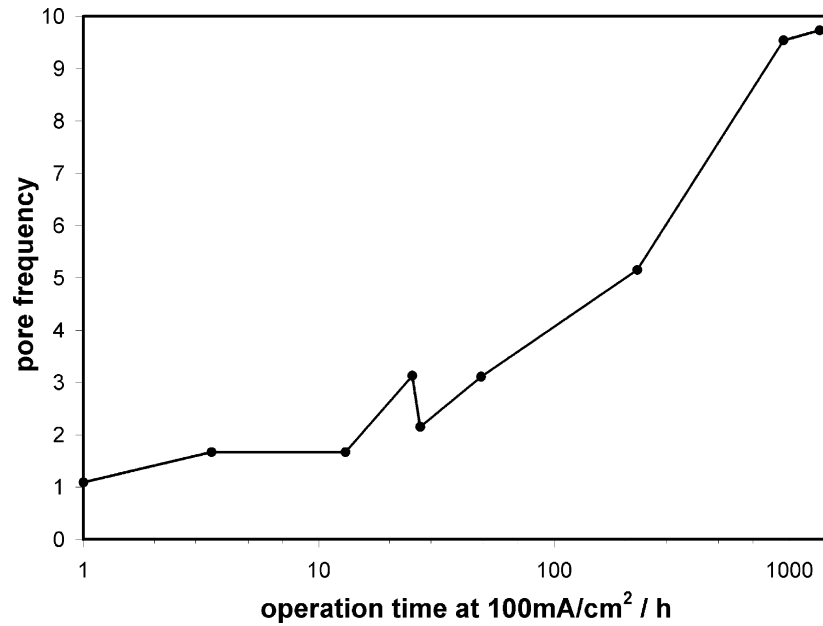


Fig. 7. Recorded pore frequency as function of the operation time of the electrodes.

compared with the single crystalline phases. Therefore, we conclude that the increasing of the pore frequency during the fuel cell operation is induced by the disintegration of the Raney-nickel particles and formation of new pores on the fractured surface.

The hydrogen-induced embrittlement is caused by the hydrogen loading and de-loading of the nickel catalyst; therefore, the electrochemical conditions influence the hydrogen loading or de-loading. Finally, the disintegration of the nickel catalysts can also depend on the operation conditions like the operating current density.

Caused by the disintegration of the nickel particles, more grain boundaries are formed, and therefore poor electrical contacts between the particles should yield an increasing electrical resistance, which results in higher losses, but the most significant effect is that the potential differences in the electrodes increase and so the three-phase zone may be less extended and the electrochemical performance decreased.

In Fig. 9, the correlation between the final reciprocal surface specific conductivity, which means the reciprocal value of the last determined surface specific conductivity towards the end of the electrochemical experiment, and the

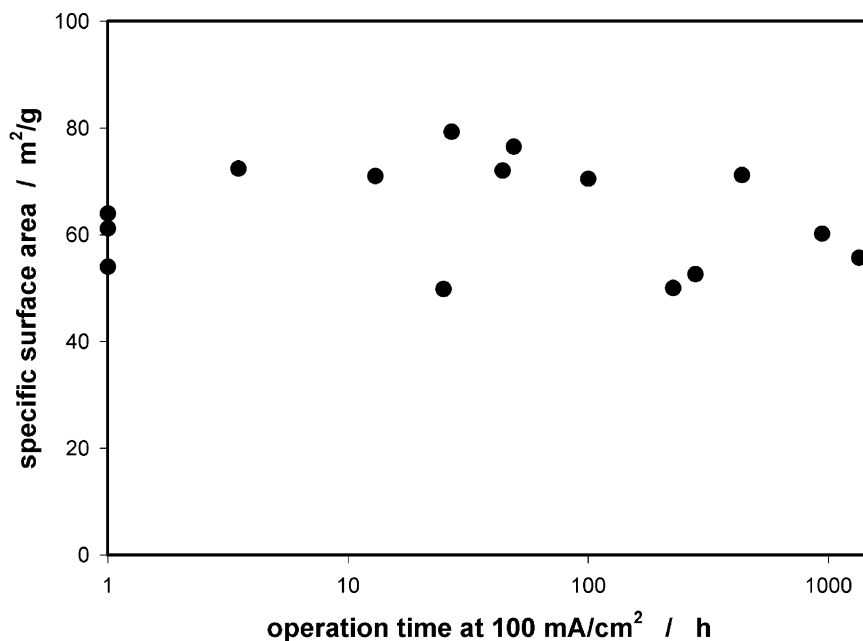


Fig. 8. Specific surface area recorded by nitrogen adsorption measurements of electrodes after various operation times at 100 mA/cm².

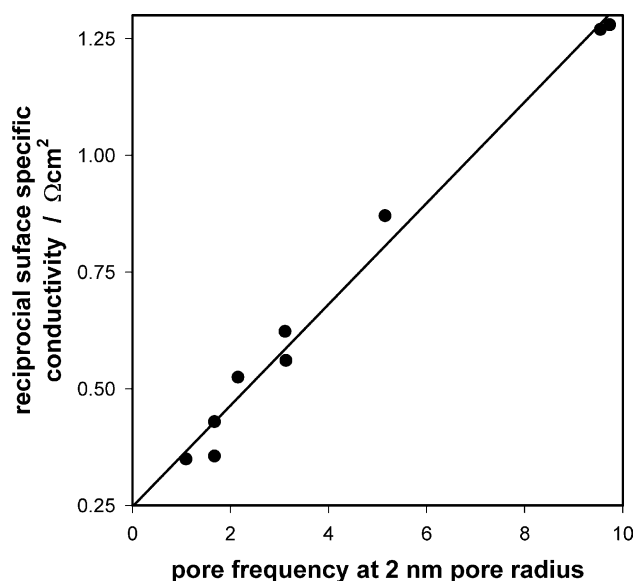


Fig. 9. Correlation between the final reciprocal surface specific conductivity and pore frequency at 2 nm of the electrodes after various operation times at 100 mA/cm².

pore frequency is displayed for the electrodes stressed at 100 mA/cm². It can be clearly seen that both parameters are strongly correlated.

4. Conclusion

For the fuel cell operation, the long-term behavior of the electrochemical performance is important. The electrochemical performance of the investigated nickel anodes decreases during the electrochemical operation, whereby the time dependence of the electrochemical performance can be described by two exponential functions with different time constants. One of the time constants is independent of the current density (time constant, 250 h), the other depends strongly on the current density. The current density depending time constant depends exponentially on the current density.

The physical characterization shows different alterations within the electrodes. The change of the added copper in the electrodes seems not to effect the electrochemical performance. The PTFE decomposes during electrochemically stressing and influences the electrochemical behavior of the electrodes, but an effect directly on the electrochemical performance cannot be observed. The nickel catalyst particles disintegrate during fuel cell operation as it can be seen in the pore size distribution and in the SEM images. The change of the pore frequency as parameter for the nickel particle disintegration and the surface specific conductivity are strongly correlated. So, it can be concluded that the disintegration of the nickel particles is the determining step for the decrease of the electrochemical performance. In addition, the nickel surface can be partially passivated by the formation of nickel oxides. We presume that the disintegration of the

nickel catalyst is induced by the hydrogen induced embrittlement of nickel.

To improve the long-term stability of the anodes, a different catalyst should be used which has a more stable structure. Therefore, the modified nickel powders used in nickel hydride accumulators seem to be interesting as catalysts in AFC, and they should be tested and investigated to determine the electrochemical activity for the hydrogen oxidation and stability under AFC conditions, because these materials are developed for reversible charging and discharging processes with hydrogen. Therefore, these materials should have a higher resistance against hydrogen-induced embrittlement than pure nickel, and may be a base material for the development of more stable nickel catalysts for AFC anodes.

References

- [1] Daimler-Benz, High Tech. Report, 1997, p. 20.
- [2] K. Kordesch, G. Simader, Fuel Cells and Their Applications, VCH Verlag, Weinheim, 1996.
- [3] E. Gülzow, N. Wagner, M. Schulze, J. Power Sources 127 (2004) 243.
- [4] S. Gultekin, M.A. Al-Saheh, A.S. Al-Zakri, K.A.A. Abbas, Int. J. Hydrogen Energy 21 (1996) 485.
- [5] Y. Kiros, S. Schwartz, J. Power Sources 87 (2000) 101.
- [6] M.A. Al-Saleh, A.S. Al-Zakri, S. Gultekin, J. Appl. Electrochem. 27 (1997) 215.
- [7] M. Schulze, K. Bolwin, E. Gülzow, W. Schnurnberger, Fresenius J. Anal. Chem. 353 (1995) 778.
- [8] E. Gülzow et al., PTFE bonded gas diffusion electrodes for alkaline fuel cells, in: Proceedings of the Ninth World Hydrogen Energy Conference, Paris, 1992, p. 1507.
- [9] A. Khalidi, B. Lafage, P. Taxil, G. Gave, M.J. Clifton, P. Cezac, Int. J. Hydrogen Energy 21 (1996) 25.
- [10] M. Schulze, E. Gülzow, G. Steinhilber, Appl. Surf. Sci. 179 (2001) 252.
- [11] N. Wagner, E. Gülzow, M. Schulze, W. Schnurnberger, Gas diffusion electrodes for alkaline fuel cells in solar hydrogen energy, in: H. Steeb, H. Aba Oud (Eds.), German-Saudi Joint Program on Solar Hydrogen Production and Utilization Phase II 1992–1995, ISBN 3-89100-028-6, Stuttgart, 1996.
- [12] E. Gülzow, M. Schulze, G. Steinhilber, J. Power Sources 106 (2002) 126.
- [13] H. Sauer, German Patent DE 2 941 774 (CI H01M4/88).
- [14] A. Winsel, German Patent DE 3 342 969 (CI C25B11/06).
- [15] E. Gülzow, K. Bolwin, W. Schnurnberger, Dechema-Monographien Bd. 117 (1989) 365.
- [16] E. Gülzow, W. Schnurnberger, Dechema-Monographien Bd. 124 (1991) 675.
- [17] E. Gülzow, K. Bolwin, W. Schnurnberger, Dechema-Monographien Bd. 121 (1990) 483.
- [18] E. Gülzow, K. Bolwin, W. Schnurnberger, Dechema-Monographien Bd. 117 (1989) 365.
- [19] E. Gülzow, K. Bolwin, W. Schnurnberger, in: Brennstoffzellen, Hrsg. H. Wendt, V. Plzak (Eds.), VDI-Verlag, Düsseldorf, 1990.
- [20] E. Gülzow, B. Holzwarth, M. Schulze, N. Wagner, W. Schnurnberger, Dechema-Monographien Bd. 125 (1992) 561.
- [21] Sleem-Ur-Rahman, M.A. Al-Saleh, A.S. Al-Zakri, S. Gultekin, J. Appl. Electrochem. 27 (1997) 215.
- [22] E. Gülzow, et al., Fuel Cell Bull. 15 (December) (1999) 8–12.
- [23] D. Bevers, E. Gülzow, A. Helmbold, B. Müller, in: Proceedings of the Fuel Cell Seminar on Innovative Production Technique for PEFC Electrodes, Orlando, FL, 1996, p. 668.

- [24] A. Helmbold, German Patent DE 197 57 492 A 1 (1999).
- [25] D. Bevers, N. Wagner, German Patent DE 195 09 749 C2.
- [26] E. Gülzow, A. Helmbold, T. Kaz, R. Reißner, M. Schulze, N. Wagner, G. Steinhilber, J. Power Sources 86 (2000) 352.
- [27] G. Ertl, J. Küppers, Low Energy Electron and Surface Spectroscopy, VCH Verlag, Weinheim, 1985.
- [28] S.J. Gregg, K.S.W. Sing, Adsorption, Surface Area and Porosity, Academic Press, London, 1982.
- [29] E. Gülzow, M. Schulze, in preparation.
- [30] H.-W. Hoppe, H.H. Strehblow, Surf. Interface Anal. 14 (1989) 121.
- [31] C.D. Wagner, W.M. Riggs, L.E. Davis, J.F. Moulder, G.E. Muilenberg (Eds.), Handbook of X-ray Photoelectron Spectroscopy, Perkin-Elmer Corporation, Eden Prairie, Minnesota, 1979.
- [32] M. Schulze, R. Reissner, M. Lorenz, U. Radke, W. Schnumberger, Electrochem. Acta. 44 (1999) 3969.
- [33] M. Schulze, E. Gülzow, G. Steinhilber, in preparation.